Published paper
Ghosh, S., Smith, M.H. and Rap, A. (2007) *Integrating biomass, sulphate and sea-salt aerosol responses into a microphysical chemical parcel model: implications for climate studies,* Royal Society A-Mathematical Physical and Engineering Sciences, Volume 354 (1860), 2659 – 2674.

INTEGRATING BIOMASS, SULPHATE AND SEA-SALT AEROSOL RESPONSES INTO A MICROPHYSICAL CHEMICAL PARCEL MODEL: IMPLICATIONS FOR CLIMATE STUDIES

S. GHOSH, M.H. SMITH and A. RAP

SCHOOL OF EARTH AND ENVIRONMENT, UNIVERSITY OF LEEDS, LEEDS LS2 9JT, U.K.

Abstract

Aerosols are known to influence significantly the radiative budget of the earth. Although the direct effect (whereby aerosols scatter and absorb solar and thermal infra-red radiation) has a large perturbing influence on the radiation budget, the indirect effect, whereby aerosols modify the microphysical and hence the radiative properties and amounts of clouds, poses a greater challenge to climate modellers. This is because aerosols undergo chemical and physical changes while in the atmosphere, notably within clouds, and are removed largely by precipitation. The way in which aerosols are processed by clouds depends on the type, abundance, and the mixing state of the aerosols concerned. A parametrization with sulphate and sea-salt aerosol has been successfully integrated within the Hadley Centre General Circulation Model (GCM). The results of this combined parametrization indicate a significantly reduced role, compared to previous estimates, for sulphate aerosol in cloud droplet nucleation, and consequently, in indirect radiative forcing. However, in this bi-component system the cloud droplet number concentration, N_d, (a crucial parameter that is used in GCMs for radiative transfer calculations) is a smoothly varying function of the sulphate aerosol loading. Apart from sea-salt and sulphate aerosol particles, biomass aerosol particles are also present widely in the troposphere. We find that biomass smoke can significantly perturb the activation and growth of both sulphate and sea-salt particles. For a fixed salt loading, N_d increases linearly with modest increases of sulphate and smoke masses, but significant non-linearities are observed at higher non sea salt mass loadings. This non-intuitive N_d variation poses a fresh challenge to climate modellers.

1. Introduction

Recent research on the impact of natural and anthropogenic aerosol on global climate indicates that sulphate aerosol particles mainly have a cooling effect because they are effective reflectors of solar radiation, and absorb very little of the incident radiation. Estimates of the aerosol direct effect on climate vary but global averages are generally between 0 and -1 Wm^{-2} for present day conditions (IPCC, 2001). Since aerosols have short lifetimes ($\sim$ a few days), their radiative forcing tends to peak and localise close to source regions. Although the most prominent source regions are Europe, North America, and SE Asia, certain parts of central Africa and South America are also strong source regions of aerosol particles due to increased biomass burning. Although the likely impact of sulphate aerosol on climate has been studied recently (IPCC), the impact of biomass aerosol had not received much attention until large scale campaigns such as ACE-Asia and INDOEX were launched.

Biomass burning make a significant contribution to atmospheric trace gases and aerosol particles on both local and global scales. Andreae et al (1996) have estimated that biomass burning could be responsible for as much as 45% of the global emissions of black carbon, which is an efficient absorber of solar radiation. Secondly, smoke particles can also act as cloud condensation nuclei (CCN). It was observed that 80-100% of the particles emitted during vegetation fires in California could act as CCN (Rogers et al. 1991). Cloud reflectivity is changed in the presence of biomass burning and the subsequent release of aerosol particles, causing changes in the albedo of tropical regions during the biomass burning season. Roberts et al (2003) found that, in the Amazon basin during the dry season, smoke aerosol from biomass burning dramatically increased CCN concentrations. Further, they found that light-absorbing substances in smoke darken the Amazonian clouds and reduce the net radiative forcing. A comparison of the Advanced Very High Resolution Radiometer (AVHRR) analysis and their modelling studies suggests that the absorption of sunlight due to smoke aerosol may compensate for about half of the maximum aerosol effect. In accordance with our own study, they also found that subtle differences in the chemical and physical makeup are particularly influential in the activation and growth behaviour of the aerosol. They further concluded that knowledge of the CCN spectrum alone is not sufficient to fully capture the climatic influence of biomass burning.

A significant improvement in model studies was achieved when the importance of sea-salt within an air mass comprising of sulphate aerosol particles was recognised (Jones et al 2001; O'Dowd et al 1999a-

b; Smith et al 1996). It was found that, when a second aerosol such as sea-salt is included, it has the potential to perturb the droplet activation process. The resultant values of N_d varied noticeably when sea salt aerosol particles were included. The effect of sub-cloud aerosol on cloud droplet concentration was explored over the North Atlantic and East Pacific under a variety of low and high wind speed conditions. A bi-component aerosol-droplet parametrization for use in GCMs was developed to predict cloud droplet number concentration as a function of sea-salt and non-sea-salt sulphate nuclei. These studies demonstrated that the effect of enhancing an existing non-sea-salt sulphate cloud condensation nuclei population with sea-salt nuclei is to reduce the number of cloud droplets activated under high sulphate conditions and to increase the cloud droplet concentration when sulphate levels are low. Ghan et al (1998) also showed that the total number concentration of activated cloud droplets increases with increasing sea-salt concentration if sulphate number concentrations are relatively low and updraughts are strong, but it decreases with higher sea-salt if sulphate number concentrations are high and cloud updraughts are weak. This is due to the activation of accumulation mode sea-salt particles, while the decrease arises from the reduction in maximum cloud supersaturation due to competition with coarse mode sea-salt particles. These conclusions are insensitive to sulphate size distribution and surface wind speed.

Modellers now recognise the fact that aerosol activation and cloud processing effects are complex and should be effectively integrated within global aerosol-climate model studies (Roelofs et al 2006). In a recent study Fountoukis and Nenes (2005) have developed parametrizations to include sulphate and sea-salt aerosol. Their formulation allows for a lognormal representation of aerosol size distribution and includes a size-dependent mass accommodation of water vapour. However, no studies have been reported to date where the aerosol activation process has been examined when three components, i.e. sulphate aerosol, sea-salt, and biomass aerosol, are included. In this study we have examined in detail the modulation of the activation process when multiple aerosol components (more representative of a real atmosphere) are present. For the first time, we have studied with repeated model runs, how N_d varies with various mass loadings of the three components.

2. An overview of the microphysical chemical parcel model

A detailed micro-physical chemical parcel model was the main tool used (O'Dowd et al 1999a). The original model could account for only pure externally mixed sulphate and sea-salt aerosols. This model was updated and altered to include biomass smoke particles which were assumed to be internally mixed with sulphate aerosol material.

The chemical model used is, in essence, a Lagrangian parcel model with explicit micro-physics utilising the dynamic growth equation (Pruppacher and Klett, 1997) to model the growth of aerosol solution droplets by condensation of water vapour on to a size-resolved droplet spectrum. Rather than being fixed, the boundaries of these size channels move as the solution droplets grow. The growth law includes curvature and solution effects, and is corrected for the breakdown of the continuum approximation close to the droplet surface (Pruppacher and Klett, 1997). Mass-transport limitations based on Schwartz (1986) have also been included. The aqueous phase chemical aspects of the model consists of (i) an equilibrium module, (ii) a kinetic reaction module, and (iii) the non-ideal behaviour correction module (Pitzer, 1991). The equilibrium module is used to calculate the amount of soluble gaseous species dissolved in the aerosol, and to apportion the aqueous aerosol species between the various associated as well as dissociated forms, which is achieved by solving the charge balance equation for each droplet. Although there are a number of similar models in existence, the present Pitzer model is one of the most advanced of its kind. Apart from including all the standard features of droplet growth considered by all microphysical models, it also takes account of high ionic strength, non-ideal solution effects. These effects impact aqueous phase chemical equilibria via Henry's law.

The kinetic reaction module is used to compute the rate of heterogeneous sulphate production in the solution droplets and sulphate production is allowed to occur by SO_2 oxidation using dissolved H_2O_2 and/or O_3 as the oxidant. The reaction rates and their temperature dependence are taken from Ayers and Larson (1990). Sources of atmospheric sulphur are DMS (dimethyl sulphide) in the ocean and gaseous SO_2 from anthropogenic emissions as well as from biomass smoke. These species are quickly transformed to sulphate, either in the nucleation mode or in the accumulation mode (Seland and Iversen, 1999). Some of the nucleation mode particles coagulate on pre-existing background aerosol to form accumulation mode particles so important to the aerosol indirect effect. The second contribution to accumulation mode sulphate comes

from SO_2 oxidation in clouds followed by evaporation, and recent sensitivity tests have shown this latter sulphate component to be more effective than the former as far as the second indirect effect is concerned (Seland and Iversen). For these reasons, it was very important to include the kinetic reaction module in our model simulations. Further details of the model can be found in O'Dowd et al (1999a).

3. Model performance and testing : consolidation of observational studies from ACE-2

Prior to configuring the micro-physical model for multiple components, it was necessary to first assess the model performance with just ammonium sulphate and sea-salt. The rationale behind this approach is two-fold : first, the performance of the chemical parcel model could be tested with observational data from ACE -2 (Aerosol Characterisation Experiment), and secondly, the biomass aerosol signature on the cloud optical properties could be singled out from model runs. ACE-2 measurements were also used to initialise the model, because the data pertain to stratocumulus clouds which contribute significantly to the aerosol indirect effect owing to their extensive coverage. We have used results for the C-130 flight A550 (25 June 1997) corresponding to a clean air mass for our base runs and thereafter simulated the biomass smoke effects as an added component.

First, we examined the accuracy of the heterogeneous cloud processing by comparing the masses of SO_4^{-2} and NH_4^+ in the fine mode. The modelled values for SO_4^{-2} and NH_4^+ are 0.069 ppb and 0.150 ppb compared to the observed values of 0.109 ppb and 0.157 ppb, respectively, for the two ionic species. Allowing for the experimental errors associated with the counting of the smallest cloud droplets by the FSSP (Forward Scattering Spectrometer Probe), the model predictions are very satisfactory - the predictions and the observations are broadly comparable. The under prediction in the sulphate mode can be partly attributed to the fact that observations (Osborne 2001 (private communication)) showed that some of the fine mode sea-salt particles were internally mixed with some sulphate material which was not accounted for by the model. However, for the relatively clean stratocumulus like conditions, it is unlikely that the N_d values (the only variable directly used by climate models) can change because the sea-salt aerosol number concentrations are significantly smaller than the sulphate aerosol concentration. It is important to note that the SO_4/NH_4 ratio ~ 0.5 - this indicates an encouraging model performance. In Table 1 we have also shown the observed and modelled values of the droplet number concentration N_d. The figure quoted corresponds to an average of all droplets with diameter $2 < D < 19\mu m$ (aerosol particles with diameters less than 2 μm are not counted as 'cloud droplets' and the number concentrations corresponding to diameters greater than 19 μm are negligible). In Table 1 we have used N_d values at 90m above cloud base but well below the cloud top at 350m, where cloud top entrainment effects are minimal, yet much of the initial sub-micron aerosol particles have diameters exceeding 2 μm. Considering the fact that there are large error bars in the observations, the modelled N_d values agree favourably with the observations. In addition, some optical properties including the maximum and minimum effective diameters, D_{eff}, and the optical thickness, τ, were also compared with the C-130 observations (Osborne et al 2000; Osborne 2001 (private communication)). A general way of estimating the cloud optical depth τ is given by

$$\tau = \frac{3}{2} \int \frac{q_l(z)}{\rho_w r_e(z)} dz \tag{1}$$

where ρ_w and q_l are the liquid water density and the LWC, respectively, and the integration extends from the cloud base to the cloud top. The above equation for solar visible wavelengths is strictly valid only for a non-absorbing medium where the drop size is much bigger than the wavelength. r_e is the droplet effective radius which is the ratio of the third to the second moment of the size spectrum. The optical properties tabulated in Table 1 provide an extremely encouraging comparison. The marginal over prediction of τ is due to the over prediction in the liquid water content (LWC) -this is to be expected in the non-entraining parcel model. Entrainment of dry air has a tendency to lower LWC which is not treated by the model. A detailed study of the chemical processing and optical properties of the ACE-2 stratocumulus for moderately polluted conditions and with the effects of cumulus penetrations has recently been published by Ghosh et al (2005b). From this latter study, we observe that model results compare extremely favourably with the observations.

By modelling the ACE-2 case study (involving two aerosol types), we demonstrate that the microphysical model is robust, and is amenable to further improvement to include multiple aerosols as well as the effects of internal mixing. Thus, this altered model provides a valuable tool for further studies to relate cloud droplet number concentrations to aerosol masses. These aspects are detailed in the subsequent sections.

4. Tri-component model simulations : biomass smoke activation along with sulphate and sea-salt aerosol

For biomass smoke particles to activate into cloud droplets, it is essential that these particles have some water soluble components (hereafter designated by the parameter ϵ). Only a limited amount of observational data are available regarding the extent of soluble material present in biomass smoke particles. Sulphates, sodium chloride, and other water-soluble salts and inorganic acids are common to the atmospheric aerosols and to CCN. The abilities of these species to serve as CCN are relatively well known, whereas our understanding of the ability of biomass smoke particles and other organic species, to act as CCN is relatively poor and is a critical area of uncertainty in global scale modelling of cloud droplet nucleation. Aerosols from biomass burning are primarily composed of organics and may act as CCN, but some of their CCN activity may actually be due to co-resident inorganic constituents (Van Dinh et al 1994; Novakov and Corrigan, 1996; Leaitch et al 1996). Measurements from a forested area suggest that biomass burning releases terpene, pinene and other organic acids and some of the products of terpene oxidation may serve as CCN (Leaitch, 1999). Virkkula et al (1999) found that particles from pinene oxidation absorbed some water at a RH of about 84%. Cruz and Pandis (1997) examined the CCN activity of particles of adipic and of glutaric acid (products of alkene oxidation) and found reasonable agreement with Kohler theory, whereas Corrigan and Novakov (1999) measured much higher activation diameters than predicted by theory.

The preceding discussions suggest that accounting for all the chemical species in biomass smoke particles in a numerical model may be intractable. However, since we are more concerned with the physico-chemical properties which significantly affect the activation of these particles into cloud droplets, we assume that inorganic sulphate comprises the major contributor to the amount of soluble material in biomass smoke particles. Among recent observational studies of biomass smoke particles, that conducted by Yamsoe et al (2000) provides useful information not only on the chemical composition of these particles, but also estimates the amount of soluble material to be expected within these particles. The Yamosoe et al study was concerned with aerosol particles sampled directly over freshly-emitted biomass burning plumes, very close to the sources (about 0.5-2 m away from the fire) to characterise direct emissions. From the Yamasoe et al study amount of soluble sulphate material present ~ 0.25 and this is appropriate for biomass particles that are slightly aged to include some sulphate material. Elemental composition and water soluble ionic components are reported by Yamasoe et al only for the fine aerosol mass fraction. This fraction comprises most of the aerosol emissions and corresponds to the most interesting particles for climate change due to their long atmospheric residence time and optical properties. Further details of the experimental procedures can be obtained from Yamsoe et al. We also assumed that the soluble mass fraction comprised only sulphates and that this mass fraction was representative of both flaming and smoldering emissions. We have however, performed sensitivity tests to study the N_d dependence on ϵ. We examined the cloud droplet spectrum at 90 m above the cloud base for $\epsilon = 0.05, 0.25$ and 0.6, corresponding to relatively fresh, moderately aged, and fully aged biomass particles at moderate levels of aerosol mass loadings. We find that with increasing values of ϵ the spectrum broadens to larger sizes. For $\epsilon = 0.05$ and 0.25 we obtain a mono modal spectrum with maximum N_d centred around a droplet diameter of $11 \mu m$ but with a broader spectrum for the latter case. For the fully aged case ($\epsilon = 0.6$) a second peak develops around a droplet diameter of 13 μm in addition to a first peak centred around a diameter of 9 μm, indicating an even broader droplet spectrum. However, most importantly, the total N_d sums up to a value of approximately 177 cm^{-3} in all the three cases. Since the total N_d does not change with increasing values of ϵ, we can conclude that parametrised N_d values generated from multiple model runs can be effectively used in host climate models without any loss of generality. In our subsequent analyses, we shall only discuss results corresponding to $\epsilon = 0.25$.

Finally, for the sake of completeness it is important that we also briefly discuss the likely impacts of soot or black carbon which can also be present along with biomass particles. Soot carbon particles have a much smaller median radius and are less soluble. The Hadley Centre recommends a median radius of 40 nm which is approximately a third of the biomass median radius. Both soot and biomass aerosol particles have comparable densities and therefore with comparable mass loadings, sensitivity studies show that biomass particles have a greater influence on the overall N_d values when present with sulphate and sea salt aerosol. However, in situations where soot carbon mass overwhelms biomass aerosol mass, the N_d values are perturbed by soot aerosol. Work is in progress to develop parametrisations with many possible combinations of sulphate, sea salt, biomass and soot carbon.

Many more sensitivity tests are, of course, necessary to elucidate all the mechanistic details pertaining

to fresh and aged smoke in both flaming and smoldering conditions, as well as the presence of other soluble organic constituents in the air masses. Thus, these results should be regarded as a current best approximation with the estimated sulphate fraction being a reasonable proxy for other hygroscopic components.

4.1 Model configuration

Before configuring the model to include biomass smoke along with sulphate aerosol and sea-salt, it is necessary to examine, in particular, how the soluble fraction of the biomass smoke affected the activation of cloud droplets when internally mixed with ammonium sulphate.

In this study, we have not looked at surface tension effects because we have assumed that the solution is still very dilute, so that the surface tension is similar to that for water droplets. Furthermore, electrolyte concentrations in recently-activated CCN typically are not large enough to induce a significant change in surface tension (Pruppacher and Klett, 1997). However, although a smoke particle may be treated as partially inert (e.g. a pure externally mixed smoke particle), it can contribute to a particle's size which affects the Kelvin term in the Kohler equation. Similarly, we have not altered the value of the mass accommodation coefficient since, for dilute solutions, it is expected that the value should be close to unity (Wagner 1982).

Some model configuration was necessary to study the effect of the biomass solubility on the droplet activation. The solubility term appears in the expression for the hygroscopicity in the Kohler theory :

$$B = \nu \phi_s \epsilon M_w \rho_t / (M_{ap} \rho_w) \tag{2}$$

where ν=number of ions the salt dissociates into within water, ϕ_s = osmotic coefficient ($\sim$ 1), ϵ=mass fraction of the soluble material, M_w = mol. wt. of water, M_{ap}=mol. wt of aerosol particle, ρ_w=density of water.

Clearly, when the fraction of the soluble material in the aerosol particle changes, a corresponding change in the density of the aerosol particles results, which has to be appropriately apportioned. This is done by calculating ρ_t, the effective density with soluble and insoluble material, and can be expressed as

$$\rho_t = \rho_s * \rho_{insol} / (\rho_s - \epsilon(\rho_s - \rho_{insol}))$$

where ρ_s = density of soluble material (ammonium sulphate 1769 kg/m^3), ρ_{insol}= density of insoluble material (smoke 1350 kg/m^3).

It is important to note that B depends on aerosol composition, which determines the number of ions, ν, the mass fraction of the water soluble substance, ϵ, the particle material density, and the molecular weight. Thus, from the above equations, we find that B increases when ϵ increases or when ν increases, assuming that the osmotic coefficient remains unchanged.

The amount of water vapour available during the growth process is strongly dependent on various dynamical aspects and the particle size distribution. Particles carrying more hygroscopic material consume more water vapour during their growth before reaching the maximum saturation. The maximum saturation ratio reached is typically smaller in the case when we have more soluble material in the nascent droplets than in the case when we have less soluble material in the droplets.

4.2 Microphysical model input parameters

The chemical parcel model was configured with log-normal input aerosol spectra from data currently in use by the U.K. Met. Office (UKMO). Sea-salt observations (O'Dowd et al 1999c) reveal that the distribution is spread over a fine film mode along with a coarser jet mode. We have allowed the dry aerosol input spectra to correspond to 3 components with 4 modes - pure ammonium sulphate, fresh biomass smoke, sea salt (film mode) and sea-salt (jet mode). The chosen aerosol-mass ranges include low to moderate mass loadings of sulphate and smoke which respectively correspond to clean and moderately polluted urban conditions. Thus, the activation scenario becomes a multi-dimensional problem with the mass components of the individual species and the resultant N_d forming the components of a multi-dimensional space. Our results (see section 5) clearly indicate that a linear increase of one component mass in one direction does not necessarily evoke a linear response in N_d.

The spectral properties of ammonium sulphate, biomass smoke, and sea-salt are shown in Table 2a.

The concentration of sea-salt particles is highly wind-speed dependent and is parametrized by the method outlined by O'Dowd et al (1999c), which is described by the following equations :

$$Log_{10}N_{film} = 0.095U_h + 6.283, \quad (3)$$

$$Log_{10}N_{jet} = 0.0422U_h + 5.7122. \quad (4)$$

N_{film} and N_{jet} are the sea-salt particle concentrations in the film and jet modes, expressed in units of particles m^{-3} and U_h is the horizontal wind speed in ms^{-1}. The above equations are valid for $2 < U_h < 17.5ms^{-1}$ and this range covers the range of wind speed values observed by the UKMO (O' Dowd et al 1999c)

Table 2b lists the trace gas concentrations and the dynamical inputs, both based on the C-130 measurements from the ACE-2 campaign. In addition to the ACE-2 data set, we also examined the distributions of vertical velocity near the cloud base of a marine stratocumulus that developed off the coast of California (David Roberts, private communication). Based on these two data sets it was inferred that a choice of the most probable updraught velocity $\sim 0.2ms^{-1}$ is appropriate for our runs.

We have however undertaken sensitivity studies where we estimated N_d as a function of varying updraught speeds. We found that at low updraught speeds, when $U < 0.2ms^{-1}$ the N_d values increased rapidly with increasing U - $N_d \sim 70cm^{-3}$ at $U \sim 0.1ms^{-1}$, and increased rapidly to 120 cm^{-3} when $U \sim 0.15ms^{-1}$. However, for $0.2 < U < 0.5ms^{-1}$, N_d values ranged between 175-200 cm^{-3}, indicating a much slower rate of increase. For higher updraught speeds, when $0.5 < U < 2.0ms^{-1}$, the N_d values hardly changed from a value of 200 cm^{-3}, indicating that higher values of U can only increase N_d by approximately 10%. .

5. Aerosol activation in a tri-component domain comprising sulphate, sea salt and biomass smoke

Although, the cloud droplet number concentration N_d is a function of 3 components, the variation of N_d is presented as a function of two components with the third set at specific values. This approach not only facilitates visualisation, but also gives a deeper insight into the aerosol activation process.

In Figures 1 and 2 we have shown contours of N_d as a function of sulphate and smoke mass loadings at two different salt mass loadings, i.e 10.287 and 27.646 μgm^{-3}. We observe that the overall number concentrations are largely controlled by the non-sea-salt aerosol. N_d increases linearly with increasing sulphate and smoke masses only for modest values of sulphate and smoke mass loadings. A strong non-linearity is observed beyond a smoke aerosol mass threshold $\sim 1.5\mu gm^3$ in both Figures. This is due to the increase in competition for the available water vapour in the air parcel - when there is a preponderance of aerosol particles competing for a limited amount of water vapour, the supersaturation decreases and some of the aerosol particles are not able to grow into cloud droplets, resulting in a fall in N_d values. The effect of increased levels of salt masses is illustrated by comparing Figures 1 and 2. Introduction of higher levels of salt can also result in a decrease in N_d values, particularly at modest sulphate and high smoke mass levels.

In Figures 3 and 4 we have shown the N_d variations as a function of smoke and salt masses for modest (Figure 3) and high levels (Figure 4) of smoke mass. In Figure 3, we notice that at all levels of sulphate masses, the contour lines are slightly inclined to the left. This clearly indicates that at this level of smoke mass loading, and for all levels of sulphate masses, N_d increases linearly with increasing salt mass loading. With the introduction of further amounts of smoke (Figure 4) the linear and predictable picture of the N_d variability completely disappears -at high levels of salt (in excess of 20 μgm^{-3}) N_d values start to fall appreciably.

The complex and often non-linear dependence of N_d on aerosol mass loadings are best illustrated by examining specific slices through the multi-component domains. We show one such slice in Figure 5. The overall higher number concentrations in Figure 5 are due to the high sulphate loading. For similar amounts of aerosol masses of the three species, our simulations indicate that sulphate aerosol particles are the most effective for elevating values of N_d. Sulphate aerosol particles yield 3 ions in an aqueous solution, are highly soluble and as a result can have a significant impact on the solubility term in the Kohler equation. In Figure 5 we clearly observe that N_d first increases linearly with increasing smoke loadings and beyond a smoke threshold of $\sim 1.5\mu gm^{-3}$, the N_d values are almost halved with further increases in the smoke mass levels.

In the preceding paragraphs we have amply demonstrated that in a multicomponent domain the activation of cloud droplets from aerosol particles is a complicated process. Although, intuitively, one would expect that that N_d should increase with increasing aerosol loadings, we have seen that this is not always true. Since

global climate models world wide use N_d-aerosol number concentration relationships in a closed parametric form for both microphysical and radiative transfer calculations, any mis-representation of N_d values are likely to induce some further uncertainties in climate predictions. It is therefore appropriate at this stage to briefly discuss some current methods employed to estimate N_d from aerosol number concentrations. The Hadley Centre currently uses a modified version of Jones et al (2001) relationship which takes sulphate, sea-salt and biomass-burning aerosols as input. Sea-salt number concentrations are obtained directly from a sea-salt parametrization (O'Dowd et al 1999b), sulphate and biomass are converted from mass concentration to number concentration assuming log-normal size distributions. All the number concentrations are then just simply added to give the input number concentration. Thus, an external mixture is always assumed. In effect, the combined relationship reduces to

$$N_d = 375(1 - exp[-0.0025A]), \tag{5}$$

where N_d is expressed in Ncm^{-3}, $A = A_{SO4} + A_{SS_{film}} + A_{SS_{jet}} + A_{biomass}$, and the '$A$'s are number concentrations of sulphate, sea-salt film and jet modes, and biomass aerosol, respectively.

In the above formulation described in equation (5) one assumes that N_d approaches a maximum value of 375 cm^{-3} asymptotically. In addition, a smooth asymptotic increase is always achieved. We have compared our N_d predictions with values obtained from (5) under similar conditions and find that equation (5) under-predicts the overall N_d values. The under prediction is more pervasive (up to $50cm^{-3}$) particularly at high aerosol mass loadings. In addition, the over simplified predictions from equation (5) also fail to capture the non-linear dependence of N_d on aerosol mass loadings. We have just described (e.g. Figures 1 and 2) that the N_d variation can be often non-linear and complex in a multi-component domain beyond certain critical aerosol mass loadings for specific components. In addition, equation (5) assumes pure external mixtures. In reality, aerosol particles, particularly over polluted urban areas and over air contaminated by forest fire emissions, are often internally mixed with various other component species. Biomass smoke observations (e.g. Yamasoe et al 2000; Okada et al 2001) indicate that these particles are generally internally mixed with some sulphate material. In an SO_2-rich polluted uban airmass, the amount of soluble sulphate material that can internally mix with a biomass aerosol particle can be high. In the present study therefore we have allowed the biomass particles to be internally mixed.

Before concluding this section, it is appropriate to discuss the implications of including many more species than the three components studied thus far. From our experience so far we can state that N_d can vary monotonically with increasing aerosol masses for a two component system comprising of sulphate aerosol and a fixed amount of sea salt. A third component, i.e. biomass aerosol, leads to a complex dependence of N_d on the aerosol masses. The anomalous dependence of N_d on aerosol loading when sea salt particles are introduced into the aerosol mixture becomes much more pronounced when additional components with differing chemical and physical characteristics are incorporated. If we add a fourth component, with similar spectral properties, we anticipate further changes provided it has enough soluble material. Under these conditions, the fourth component is likely to modulate the environmental saturation ratio on which aerosol activation is crucially dependent. Finally, sensitivity tests show that with the same median radii, when one chooses a narrower standard deviation for the log-normal spectrum, much more complex and non-linear behaviour is obtained in the N_d variations. Overall we find that a broader standard deviation has a smoothing effect on the N_d variation.

6. Wider implications and Concluding remarks

The most important result from this study is that, when sulphate aerosol, biomass smoke and sea-salt simultaneously contribute to the cloud droplet activation process, the resultant cloud droplet number concentration N_d cannot be estimated straightforwardly, as is done for situations when only sulphate and/or sea-salt aerosol are present. In a tri-component activation domain, N_d can vary in a complicated non-linear way under certain conditions, and this feature should be recognised by General Circulation Models. This will require the use of sophisticated interpolation schemes (rather than simple parametrized relationships described by equation (5)) that can accurately model the N_d variability. Such numerical schemes are essential to fully integrate the cloud droplet number concentration variability in multi-component aerosol systems (Rap et al 2006). These schemes should be numerically cost efficient, should yield an exact fit to the data generated by multiple model runs, and should include a realistic progression of interpolated values from one data point to others in its vicinity. We believe that the results presented in Figures 1-5 will aid climate

modellers worldwide to obtain reasonable estimates for N_d since the graphs cover an exhaustive range of input aerosol masses.

Our simulations show the maximum sensitivity to sulphate aerosol. The sulphate particles and some of the film mode salt particles have radii within the accumulation mode of an aerosol spectrum. These aerosols can hydrate to diameters between 0.1 to 2 μm where their mass extinction efficiency is the largest. Accumulation mode aerosols not only have high scattering efficiency, but they also have long lifetimes and very efficiently form cloud condensation nuclei (IPCC 2001). The effects of biomass smoke are sensitive to values of sulphate and sea-salt loadings.

The complex and non-linear N_d variations shown in Figures 1-5 can impact both the first and second indirect effects. The first indirect effect is modelled by allowing the cloud droplet effective radius used in radiation schemes in GCMs to be calculated from N_d-aerosol concentration parametrizations. As a result, any discrepancies in N_d estimates are likely to affect estimates of the first indirect effect. We now discuss the possible implications of this variability on the second indirect effect.

The early stages of cloud droplet growth occur by the condensation of water vapour onto CCN when the relative humidity just exceeds 100%. However, the rate of condensational growth slows as the droplets grow to larger sizes, and this process on its own cannot account for the production of precipitation-sized particles in warm clouds over the times observed (Pruppacher and Klett 1997). Precipitation formation in warm clouds is governed by a stochastic process wherby a small fraction of cloud droplets grow rapidly and have appreciable fall speeds relative to other cloud droplets. This triggers the collision-coalescence process. In GCMs this partitioning of cloud water into rain water is achieved through an 'autoconversion term'. For the same cloud water content, autoconversion is slower for a high concentration of smaller droplets than for a low concentration of larger droplets. This mechanism therefore has a large bearing on the second indirect or the lifetime effect. Autoconversion parametrizations used in some GCMs use the Tripoli and Cotton (1980) scheme which calculates an autoconversion rate and a threshold (Jones et al 2001).

When we calculated the autoconversion rates from Tripoli and Cotton (1980) and used the N_d distribution in Figure 1, we observed a significant amount of variability in the autoconversion rates - the maximum value of 9.96 $\times 10^{-7} s^{-1}$ is almost double that of the minimum value of 5.73 $\times 10^{-7} s^{-1}$. Further, autoconversion is allowed to proceed once cloud liquid water exceeds a threshold minimum and ideally this threshold q_{min} should depend on aerosol concentration. The value of q_{min} ranges from $\sim 0.005 gkg^{-1}$ in remote regions to $\sim 1.2 gkg^{-1}$ close to polluted regions in urban areas, indicating that N_d, and therefore aerosol concentration, has a double impact on autoconversion: high values not only suppress the rate, they also increase the threshold (Jones et al 2001).

There is another area of cloud microphysics that is being actively pursued world wide and which has a direct bearing on the present study - this pertains to the quantification of the settling rates of cloud droplets. In current models the cloud droplets are prescribed with still air settling speeds. In reality, clouds are turbulent and when cloud droplets settle past microscale eddies inherently present in turbulent clouds, recent calculations show that droplets with radii $\sim 10 \mu m$ do indeed settle faster than their still air fall speeds (Davila and Hunt 2001; Ghosh et al 2005a). Rogers and Yau (1989) suggest that autoconversion will only proceed once the number concentration of cloud droplets greater than 20 μm in radius exceeds approximately $10^3 m^{-3}$. When cloud droplets settle faster in turbulence, it is expected that the autoconversion process will be more efficient since the rate at which cloud droplets with radii in excess of 20 μm form will be faster. We therefore observe that autoconversion rates can be highly variable not only due to N_d variability (as in Figures 1 -5) induced by competing aerosol effects in a multi-aerosol environment, but also due to the changes induced by turbulence assisted settling rates of cloud droplets. Both these factors are important and we hope to carry these ideas forward within the framework of GCMs in the future.

Acknowledgements

We thank Lord Julian Hunt, Dr David Roberts and colleagues at the Met Office. This research was supported by the UK Department for Environment, Food and Rural Affairs under contract PECD 7/12/37.

References

Andreae, M.O., Atlas, E., Cachier, H., Cofer III, W.R., Harris, G.W., Helas, G., Koppmann R., Lacux, J.-P., Ward, D.E., 1996. Trace gas and aerosol emissions from savanna fires. In Levine, J.S. (Ed.), Biomass Burning and Global Change, Vol. 1 : Remote Sensing, Modeling and Inventory Development, and Biomass

Burning in Africa. MIT press, MA, pp. 278-295

Ayers, G.P., and Larson, T.V., 1990. Numerical study of droplet size dependent chemistry in oceanic, wintertime stratus cloud at southern mid-latitudes. *Journal of Atmospheric Chemistry*, **11**, 143-167

Corrigan, C.E., Novakov, T., 1999. Cloud condensation nucleus activity of organic compounds. A laboratory study. *Atmospheric Environment*, **33**, 2661-2668

Cruz, C.N., and Pandis, S.N., 1997. A study of the ability of pure secondary organic aerosol to act as cloud condensation nuclei. *Atmospheric Environment*, **31(15)**, 2205-2214

Davila, J., and Hunt, J.C.R., 2001. Settling of particles near vortices and in turbulence. *Journal of Fluid Mechanics*, **440**, 117-145

Fountoukis, C., and Nenes, A., 2005. Continued development of a cloud droplet formation parameterization for global climate models. *J. Geophys. Res.*,**110**, d11212, doi:10.1029/2004JD005591.

Ghan, S., Guzman, G., Abdul-Razzak, H., 1998. Competition between sea-salt and sulfate particles as cloud condensation nuclei. *Journal of the Atmospheric Sciences*, **55**, 3340-3347

Ghosh, S., Davila, J., Hunt, J.C.R., Srdic, A., Fernando, H.J.S., and Jonas, P.R., 2005a. How turbulence enhances coalescence of settling particles with applications to rain in clouds. *Proceedings of the Royal Society A*, **461**, 3059-3088

Ghosh, S., Osborne, S., Smith, M.H., 2005b. On the important of cumulus penetration on the microphysical and optical properties of stratocumulus clouds. *Atmospheric Chemistry and Physics*, **5**, 755-765

Intergovernmental Panel on Climate Change (IPCC), Climate Change 2001: The Scientific Basis-Contribution of Working Group I to the IPCC Third Assessment Report 2001, edited by Sir J. Houghton and D. Yihui, Cambridge University Press, New York.

Jones, A., Roberts, D.L., Woodgate, M., Johnson, C.E., 2001. Indirect sulphate aerosol forcing in a climate model with an interactive sulphur cycle. *Journal of Geophysical Research*, **106**, 20293-20310

Leaitch, W.R., Li, S.-M., Liu, P.S.K., Banic, C.M., Macdonald, A.M., Isaac, G.A., Couture, M.D., Strapp, J.W., 1996. Relationships among CCN, aerosol size distribution and ion chemistry from airborne measurements over the Bay of Fundy in August-September, 1995. In : Nucleation and Atmospheric Aerosols, Kulmala, M., Wagner, P. (Eds.). Elsevier Science Inc., pp. 840-843

Leaitch, W.R., Bottenheim, J.W., Biesenthal, T.A., Li, S.-M., Liu, K., Asalian, H. D.-C, Hopper, F., Brechtel, F.J., 1999. A case study of gas-to-particle conversion in an eastern Canadian forest. *Journal of Geophysical Research*, **104**, 8095-8111

Novakov, T., Corrigan, C.E., 1996. Cloud condensation nucleus activity of the organic component of biomass smoke particles. *Geophysical Research Letters*, **23**, 2141-2144

O'Dowd, C., Lowe, J.A., and Smith, M.H., 1999a. Observations and modelling of aerosol growth in marine stratocumulus-case study. *Atmospheric Environment*, **33**, 3053-3062

O'Dowd, C., Lowe, J.A., Smith, M.H., Kaye, A.D., 1999b. The relative importance of non-sea-salt sulphate and sea-salt aerosol to the marine cloud condensation nuclei population: An improved multi-component aerosol-cloud droplet parametrization. *Quarterly Journal of the Royal Meteorological Society*, **125**, 1295-1313

O'Dowd, C., Lowe, J.A., Smith, M.H. 1999c. Coupling sea-salt and sulphate interactions and its impact on cloud droplet concentration predictions. *Geophysical Research Letters*, **26**, 1311-1314

Okada, K, Ikegami, M., Zaizen, Y., Makino, Y., Jensen, J.B., Gras, J.L., 2001. The mixture state of individual aerosol particles in the Indonesian haze episode. *Aerosol Science*, **32**, 1269-1279

Osborne, S.R., Johnson, D.W., Wood, R., Bandy, B.J., Andreae, M.O., O'Dowd, C., Glantz, P., Noone, K., Gerbig, C., Rudolph, J., Bates, T., and Quinn, P., 2000. Evolution of the aerosol, cloud and boundary-layer

dynamic and thermodynamic characteristics during the 2nd Lagrangian experiment of ACE-2. *Tellus*, **52B**, 375-400

Pitzer, K.S., 1991. Activity Coefficients in Electrolyte Solutions. CRC Press. Ann Arbor.

Pruppacher, H.R., and Klett, J.D., 1997. *Microphysics of Clouds and Precipitation.* Kluwer Academic. Dordredcht.

Rap, A., Ghosh, S., Smith, M.H., 2006. Shepard and Hardy multiquadric interpolation methods for multi-component aerosol-cloud parameterisation. In preparation.

Roberts, G.C., Nenes, A., Seinfeld, J.H., Andreae, M.O., 2003. Impact of biomass burning on cloud properties in the Amazon Basin. *Journal of Geophysical Research*, **108**(D2), 4062, doi:10.1029/2001JD000985

Roelofs, G.J., Stier, P., Feichter, J., Vignati, E., Wilson, J., 2006. Aerosol activation and cloud processing in the global aerosol-climate model ECHAM5-HAM. *Atmospheric Chemistry and Physics*, **6**, 2389-2399

Rogers, C.F., Hudson, J.G., Zielinska, B., Tanner, R.L., Hallet, J., Watson, J.G., 1991. Cloud condensation nuclei from biomass burning. In Levine, J.S. (Ed.), Global Biomass Burning : Atmospheric, Climatic and Biospheric Implications. MIT press, MA, pp. 431-438

Rogers, R.R., and Yau, M.K., 1989. *A short course in cloud physics (3rd edition)*, Pergamon Press, Oxford.

Schwartz, S.E., 1986. Mass-transport considerations pertinent to aqueous phase reactions of gases in liquid-water clouds in W.Jaeschke, (ed), *Chemistry of Multiphase Atmospheric Systems, NATO ASI ser.*, Springer New York.

Seland, O., and Iversen, T., 1999. A scheme for black carbon and sulphate aerosols tested in a hemispherical scale Eulerian dispersion model. *Atmospheric Environment*, **33**, 2853-2879

Smith, M.H., Jones,A., Lowe, J.A., O'Dowd, C., 1996. Role of atmospheric aerosol in the indirect climate cooling mechanism. *Proc. 12th Int. Conference on Clouds and Precipitation*, Zurich,932-935

Tripoli, G.J. and Cotton, W.R., 1980. A numerical investigation of several factors contributing to the observed variable intensity of deep convection over South Florida. *Journal of Applied Meteorology*, **19**(9), 1037-1063.

Van Dinh, P., Lacaux, J.-P., Seroplay, 1994. Cloud-active particles from African savanna combustion experiments. *Atmospheric Research*, **31**, 41-58

Virkkula, A., Dingenen, R.V., Raes, F., Hjorth, J., 1999. Hygroscopic properties of aerosol formed by oxidation of limonene, a-pinene, and b-pinene. *Journal of Geophysical Research*, **104**, 3569-3579

Wagner, P.E., 1982. Aerosol growth by condensation, in Aerosol Microphysics II, Marlow, W.H. (Ed.), 129-178, Springer-Verlag, New York

Yamasoe, M.A., Artaxo, P., Miguel, A.H., Allen, A.G., 2000. Chemical composition of aerosol particles from direct emissions of vegetation fires in the Amazon Basin : water-soluble species and trace elements. *Atmospheric Environment*, **34**, 1641-1653

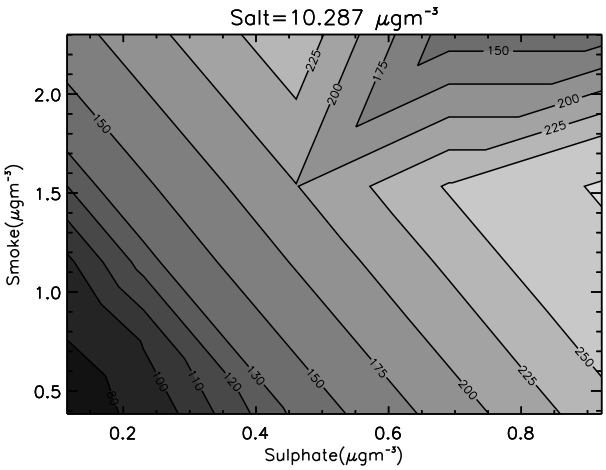

Figure 1. Variation of N_d (Ncm^{-3}) (the marked contour lines) with biomass smoke and sulphate mass for salt mass fixed at 10.287 μgm^{-3} (U_h = $5ms^{-1}$). Note the non-linear distribution at high values of smoke mass.

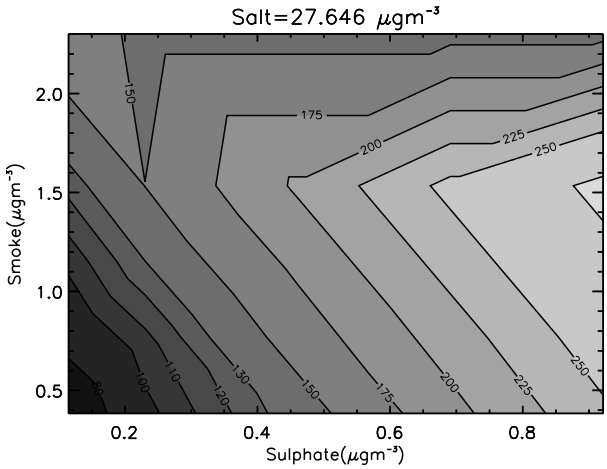

Figure 2. Variation of N_d (Ncm^{-3}) (the marked contour lines) with biomass smoke and sulphate mass for salt mass fixed at 27.646 μgm^{-3} (U_h = $15ms^{-1}$). Note that the higher salt mass has a perturbing effect on the distribution at low sulphate and high smoke levels.

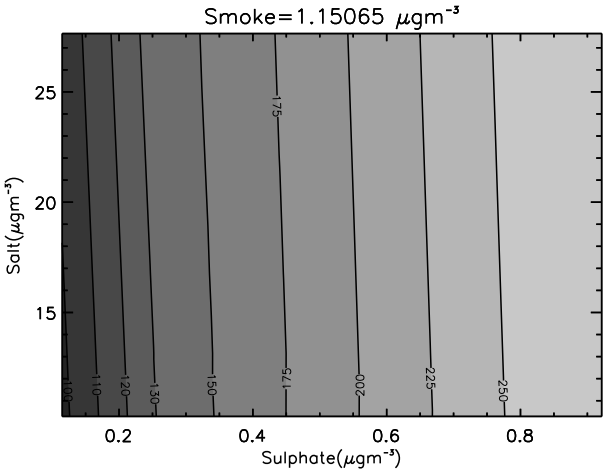

Figure 3. Variation of N_d (Ncm^{-3}) (the marked contour lines) with sulphate and salt mass for smoke mass fixed at 1.1506 μgm^{-3}. Note the linear contour lines.

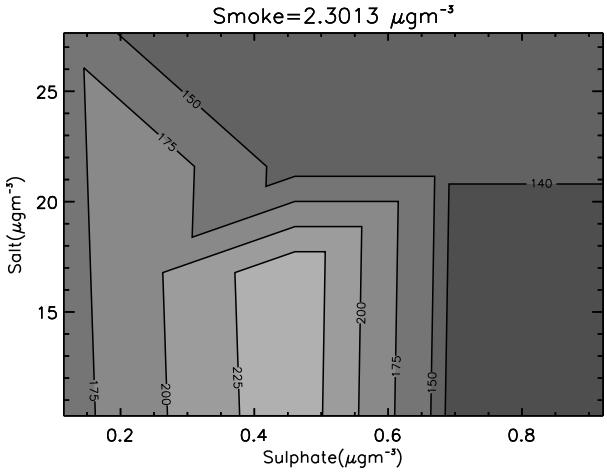

Figure 4. Variation of N_d (Ncm^{-3}) (the marked contour lines) with sulphate and salt mass for smoke mass fixed at 2.3013 μgm^{-3}. Note that the higher smoke loading induces a non-linear N_d variability.

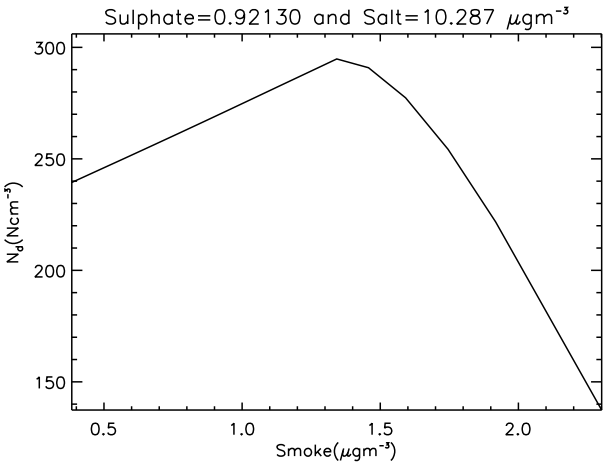

Figure 5. Variation of N_d with smoke mass for fixed salt (10.287 μgm^{-3}) and sulphate (0.92130 μgm^{-3}) masses.

Table 1 Modelled and observed microphysical and radiative properties for the ACE-2 case study

Parameter	Model	Observation
min $D_{eff}(\mu m)$	9.6	~ 8.0
max $D_{eff}(\mu m)$	27.3	22.0
$N_d\ cm^{-3}$	45.7	53 ± 20
τ	4.1	$1.9 - 3.8$

Table 2a Input aerosol spectral properties

Spectral properties	Median radius $\overline{a}$ (nm)	Standard Deviation σ	Density $\rho\ (kgm^{-3})$
Pure ammonium sulphate	95	1.4	1769
Biomass smoke	120	1.3	1350
Sea-salt (film mode)	100	1.9	2165
Sea-salt (jet mode)	1000	2.0	2165

Table 2b Input parameters for the microphysical model

Trace gas	Concentration
CO_2	350.0 (ppm)
NH_3	0.3 (ppb)
O_3	30.0 (ppb)
H_2O_2	1.0 (ppb)
SO_2	5.0 (ppt)
HCl	10^{-5} (ppt)
Dynamical variables	
Updraught speed (ms^{-1})	0.2
Relative Humidity	98.9%
Temperature	10.24 C
Pressure	879.8 mb